CHIN. PHYS. LETT. Vol. 38, No. 10 (2021) 106801

Effect of Oxide Content of Graphene Oxide Membrane on Remarkable Adsorption for Calcium Ions

Jie Jiang(江杰)[1,2], Long Yan(闫隆)[1*], and Haiping Fang(方海平)[1,3]

[1]*Shanghai Institute of Applied Physics, Chinese Academy of Sciences, Shanghai 201800, China*
[2]*University of Chinese Academy of Sciences, Beijing 100049, China*
[3]*Department of Physics, East China University of Science and Technology, Shanghai 200237, China*

(Received 6 August 2021; accepted 14 September 2021; published online 28 September 2021)

Graphene oxide membranes (GOMs), as one of the most promising novel materials, have gained great interest in the field of adsorption. However, the oxygen content of graphene oxide is directly related to its adsorption properties, such as suspension stability, adsorption capacity, and reusability of GOMs. Here, a series of reduced GOMs with oxygen content from 28% to 12% were conveniently prepared by the thermally reduced and the corresponding interlayer spacing of these membranes changed from 8.0 Å to 3.7 Å. These prepared GOMs have remarkable Ca^{2+} adsorption capacity, which increases with the oxygen content or interlayer spacing of GOMs. Importantly, the max adsorption capacity of the mass ratio between adsorbed Ca^{2+} and pristine GOMs can reach up to 0.481 g/g, which is about one order of magnitude higher than the adsorption capacity of activated sludge, magnetic Fe_3O_4, functionalized silica, zeolite molecular sieve, and other reported previously. Moreover, GOMs show excellent stability and the Ca^{2+} can be easily desorbed by water, so that the GOMs can be reused. Our previous theoretical analysis suggests that this remarkable adsorption is attributable to the strong interactions between Ca^{2+} and GO sheets, including the ion-π interactions between Ca^{2+} and aromatic graphitic rings as well as the electrostatic interaction between Ca^{2+} and oxygen-containing groups.

DOI: 10.1088/0256-307X/38/10/106801

Graphene oxide is a two-dimensional (2D) material derived from the oxidation of graphite, has attracted great interests due to their unique physical and chemical characteristics.[1–4] They show potential applications in many diverse technology fields, such as ion sieves, energy storage, water treatment and adsorption.[5–10] The performances of these applications are closely correlated to the characteristics of GO, such as its conductivity, water stability, specific surface area and adsorption performance.[10–14]

Cation-π interactions, characterized by the adsorption between various cations and π electron of aromatic rings, play a dominant role in physics, biology, chemistry and materials sciences. Hence, cation-π interactions are not negligible under the systems composed of cations and aromatic rings. Moreover, graphene oxide (GO) is rich in oxygen-containing groups, and the electrostatic interaction between ions and oxygen-containing groups also has influence on adsorption of GO.[15] The adsorption performance of GOMs should be collectively affected by their specific surface, aromatic ring structures and oxygen-containing groups. Therefore, it is important and necessary to further systematically study the factors affecting the adsorption performance of GOMs. Moreover, the adsorption of calcium ions is of great significance in water purification and treatment.

In this work, we prepared a series of reduced GOMs with different oxygen contents by thermal reduction method.[16] Remarkable amount of Ca^{2+} can be adsorbed inside these GOMs by using isothermal adsorption experiments. The adsorption capacity of Ca^{2+} inside the GOMs with highest oxygen content of 28% can reach as high as 0.481 g/g. Remarkably, the GOMs exhibited superior adsorption performance compared to other adsorbents, as the adsorption capacity of activated sludge, magnetic Fe_3O_4, functionalized silica and zeolite molecular sieve for Ca^{2+} were 0.019 g/g, 0.033 g/g, 0.041 g/g, and 0.052 g/g, respectively.[17,18] Characterization of these GOMs contained $CaCl_2$ ($CaCl_2$@GOMs) by using scanning electron microscopy (SEM) further confirmed the extensive distribution of $CaCl_2$ inside. Our x-ray photoelectron spectroscopy (XPS) and XRD results showed that the Ca^{2+} adsorption capacity of GOMs increases with the oxygen content or interlayer spacing of GOMs. It is also noted that the ions inside GOMs can be easily desorbed by water so that the GOMs can be reused. Our findings reveal the remarkable adsorption capacity inside the GOMs and the underlying mechanism based on the strong interactions between ions and GO sheets, including ion-π interactions between ions and aromatic graphitic rings as well as the electrostatic interaction between cation and oxide groups. These have potential applications in the field of water purification, ion separation, capacitor and battery.

Freestanding GOMs (GOMs)[19–25] were prepared

Supported by the National Natural Science Foundation of China (Grant No. 11675246).
*Corresponding author. Email: yanlong@sinap.ac.cn
© 2021 Chinese Physical Society and IOP Publishing Ltd

from the GO suspension via the drop-casting method. These GOMs were heat treated at 60 ℃, 90 ℃, 120 ℃, 150 ℃ and 180 ℃ for one hour to obtain reduced GOMs with different oxygen contents. These membranes were then immersed in $CaCl_2$ solutions with concentrations of 1.7 mol/L, 3.4 mol/L, 5.0 mol/L, 6.7 mol/L to obtain the corresponding $CaCl_2$@GOMs.

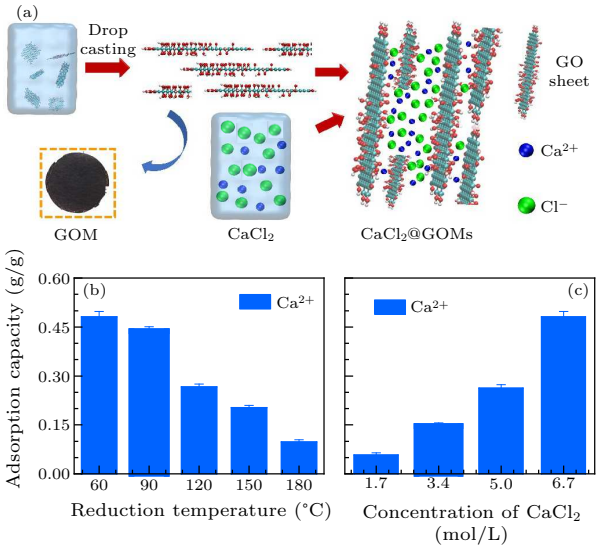

Fig. 1. Case of $CaCl_2$@GOMs. (a) Synthesis procedure of $CaCl_2$@GOMs. (b) Adsorption capacity of Ca^{2+} in $CaCl_2$@GOMs with different reduction temperatures. (c) Adsorption capacity of Ca^{2+} in $CaCl_2$@GOMs after immersing in $CaCl_2$ solution with various concentrations of 1.7 mol/L, 3.4 mol/L, 5.0 mol/L, and 6.7 mol/L. Error bars indicate the standard deviation.

We first study the $CaCl_2$ adsorption in the $CaCl_2$@GOMs with different reduction temperatures and define the adsorption capacity as the mass ratio between adsorbed Ca^{2+} and pristine GOMs. These membranes were immersed in the $CaCl_2$ solutions with concentrations of 6.7 mol/L. The metal ions in the $CaCl_2$@GOMs were determined by inductively coupled plasma optical emission spectroscopy (ICP-OES) after removal of the solution on the surface. Then, we obtained the adsorption capacity for GOMs with different reduction temperature. Figure 1(b) shows that the adsorption capacity of $CaCl_2$@GOMs is 0.481 g/g, 0.437 g/g, 0.266 g/g, 0.203 g/g, 0.098 g/g and the corresponding reduction temperature is 60 ℃, 90 ℃, 120 ℃, 150 ℃, and 180 ℃, respectively. Furthermore, the membranes reduced in 60 ℃ were then immersed in the $CaCl_2$ solution with concentrations of 1.7 mol/L, 3.4 mol/L, 5.0 mol/L, and 6.7 mol/L. The adsorption capacity of Ca^{2+} in the $CaCl_2$@GOMs increases from ∼0.058 g/g to ∼0.481 g/g with the concentration of $CaCl_2$ solution from quarter saturation to saturation [Fig. 1(c)]. Thus, the GOMs heat-treated at 60 ℃ have the max adsorption capacity ∼0.481 g/g. Remarkably, the GOMs exhibited superior adsorption performance compared to other adsorbents, as the adsorption capacity of activated sludge, magnetic Fe_3O_4, functionalized silica and zeolite molecular sieve for Ca^{2+} were 0.019 g/g, 0.033 g/g, 0.041 g/g, and 0.052 g/g, respectively [Fig. 2(a)]. The max adsorption capacity of different materials was obtained from the isothermal adsorbing experiment, and the adsorption isotherm always used to describe the quantity of adsorbate on the surface as a function of its concentration at constant temperature.

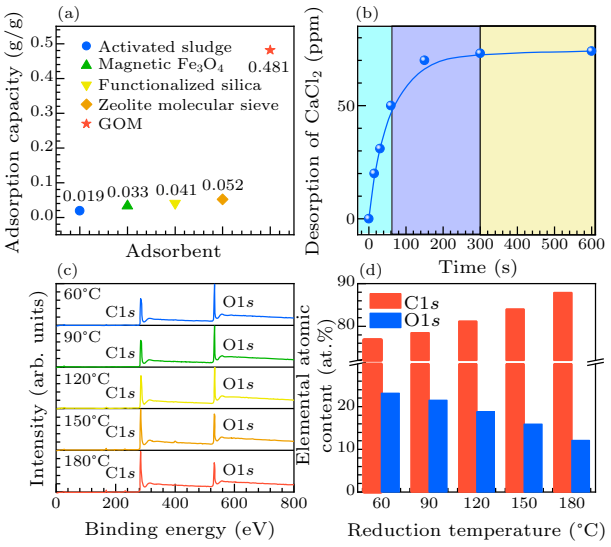

Fig. 2. (a) Adsorption capacity of different adsorbents for Ca^{2+}. (b) Desorption process of $CaCl_2$ from $CaCl_2$@GOMs after immersing in DI water of 50 mL. The process can be divided into three stages: (I) fast desorb stage (cyan-blue region), (Ⅱ) slow desorb stage (purple region), (Ⅲ) stable stage (yellow region). (c) Full-scan x-ray photoelectron spectrometer spectra of the samples of GOMs reduced in different temperatures. (d) Elemental atomic content (at.%) of C and O with respect to the reduction temperature.

While those $CaCl_2$@GOMs with the adsorption capacity of ∼0.481 g/g are immersed into deionized (DI) water, $CaCl_2$ can be easily desorbed. Figure 2(b) shows the concentrations of $CaCl_2$ after immersing in DI water. The concentration of $CaCl_2$ in the solution increases rapidly from 0 to 50 ppm in the first 1 min (stage I), and then slowly to 75 ppm in the range of 1–5 min (stage Ⅱ). Afterwards, the concentration of $CaCl_2$ becomes stable (stage Ⅲ). This indicates that the desorption process of $CaCl_2$ from the $CaCl_2$@GOMs has finished. Thus, GOMs show excellent stability in salt solution and can be easily desorbed by water, so that the GOMs can be reused.

XPS was utilized to analyze the oxygen group content. The XPS full scan spectra and C 1*s* and O 1*s* partial spectra of GOMs under different reduction temperatures are shown in Fig. 2(c). The C 1*s* and O 1*s* peak positions of reduced GOMs were at 285.08 eV and 532.08 eV, respectively. From the elemental contents of C and O in the full scan spectra, it is obvious that the oxygen content in each sample decreased sharply (from 23.2% to 12.1%) with increasing the reduction temperature from 60 ℃ to 180 ℃ [Fig. 2(d)],

indicating the successful removal of oxygen-containing groups on the GO surface.

Then, we used x-ray diffraction to analyze the reduced GOMs obtained with the different reduction temperatures. The interlayer spacings (denoted as d) of the reduced GOMs were indicated by the Bragg peaks in the XRD spectrum. There are peaks at 11.0°, 11.6°, 12.6°, 24.3°, and 24.3°, indicating that d was 8.0 Å, 7.6 Å, 7.0 Å, 3.7 Å, and 3.7 Å for the GOMs reduced at 60 ℃, 90 ℃, 120 ℃, 150 ℃, 180 ℃ membranes, respectively, as shown in Fig. 3(a). As the reduction temperature increased, the interlayer spacing of reduced GOMs decreased from 8.0 Å to 3.7 Å. This means that the interlayer spacing of GOMs is closely related to the oxygen content.

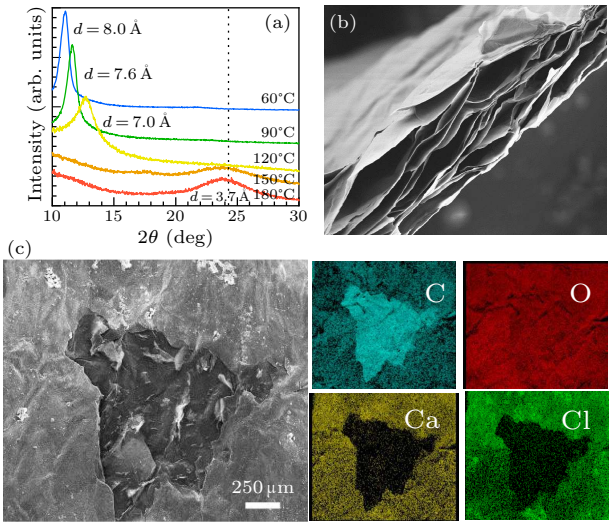

Fig. 3. (a) XRD patterns of the GOMs reduced at various temperatures. (b) Cross-sectional scanning electron microscope image. (c) Elemental mappings of $CaCl_2$@GOMs based on the SEM analysis. The elements of C, O, Ca, Cl are displayed by the colors of cyan, red, blue, and green, respectively.

Figure 3(b) shows a cross-sectional view of GOMs and Fig. 3(c) shows the SEM image of the $CaCl_2$ distribution inside the $CaCl_2$@GOMs with the adsorption capacity of ∼0.481 g/g. The elemental mappings of C, O, Ca, Cl elements are shown. We find that the signals of Ca and Cl elements in the region covered with large amount of $CaCl_2$ are shown, in much higher intensities than the intensities of C and O elements, which suggests remarkable amount of Ca and Cl elements.

Conventional porous materials without aromatic rings, such as zeolite or silica, can adsorb $CaCl_2$ for desalting or purification based on the van der Waals interaction and ion exchange mechanism. The adsorption capacity of these materials is low, resulting to the limited efficiency for practical applications. However, in our experiment, we note that the adsorption capacity of $CaCl_2$ in CaCl2@GOMs is remarkable, much larger than those in other porous materials. Different from the simple adsorption in other porous materials due to the mechanism of van der Waals interaction or ion exchange, we attribute this remarkable adsorption of $CaCl_2$ in our $CaCl_2$@GOMs to the strong interactions between $CaCl_2$ and GO sheets, including the ion-π interactions between Ca^{2+}/Cl^- and the aromatic graphitic rings as well as the electrostatic interaction between Ca^{2+} and oxide groups.

In summary, we have synthesized a series of reduced GOMs with different oxygen contents from 28% to 12% and the corresponding interlayer spacings of these membranes changed from 8.0 Å to 3.7 Å. Then, we have studied the effect of oxygen content and initial salt solution concentration on the adsorption performance of GOMs. The adsorption performance of $CaCl_2$/GOMs shows that the best adsorption effect occurs when the reduction temperature is 60 ℃, which stands for the maximum equilibrium adsorption capacity (0.481 g/g). Moreover, we find that GOMs show excellent stability in salt solution and can be easily desorbed by water, so that the GOMs can be reused.

These results are further demonstrated by our XRD pattern and confirmed by SEM experiments, and similar results are found in the adsorption process of NaCl as well (see Fig. S1 in the Supplementary Material). The key to this observation is the strong interactions between ions and GO sheets, including the ion-π interactions between ions and aromatic graphitic rings as well as the electrostatic interaction between ions and oxide groups. Our findings reveal the remarkable adsorption. Also, we have studied the effect of oxygen content and initial salt solution concentration on the adsorption performance of GOMs, which has potential applications in the fields of water purification, ion separation, capacitor and battery.

References

[1] Dreyer D R *et al.* 2010 *Chem. Soc. Rev.* **39** 228
[2] Zhu Y *et al.* 2010 *Adv. Mater.* **22** 3906
[3] Pei S and Cheng H M 2012 *Carbon* **50** 3210
[4] Yap Y K *et al.* 2013 *Chin. Phys. Lett.* **30** 024208
[5] Abraham J *et al.* 2017 *Nat. Nanotechnol.* **12** 546
[6] Joshi R K *et al.* 2014 *Science* **343** 752
[7] Xu J *et al.* 2010 *ACS Nano* **4** 5019
[8] Kuila T *et al.* 2013 *Nanoscale* **5** 52
[9] Gupta V K *et al.* 2017 *Colloid Interface Sci.* **497** 193
[10] Mo J W *et al.* 2019 *Acta Phys. Sin.* **68** 156501 (in Chinese)
[11] Hou W *et al.* 2015 *RSC Adv.* **5** 8037
[12] Nugrahenny A T U *et al.* 2014 *Carbon Lett.* **1** 38
[13] Zhang C *et al.* 2017 *Polym. Compos.* **38** E199
[14] Xi Y H *et al.* 2016 *ACS Appl. Mater. Interfaces* **8** 15557
[15] Minitha C R *et al.* 2017 *Mater. Chem. Phys.* **194** 243
[16] Zhao G K and Zhu H W 2020 *Adv. Mater.* **32** 1905756
[17] Punckt C *et al.* 2013 *Appl. Phys. Lett.* **102** 023114
[18] Meng X *et al.* 2011 *Chem. Eng. J.* **168** 737
[19] Yang Y *et al.* 2019 *RSC Adv.* **9** 3597
[20] Chen L *et al.* 2017 *Nature* **550** 380
[21] Shi G *et al.* 2018 *Nat. Chem.* **10** 7
[22] Geim A K and Novoselov K S 2007 *Nat. Mater.* **6** 183
[23] Ty Y S *et al.* 2020 *Chin. Phys. Lett.* **37** 066803
[24] Liu X and Shi G S 2021 *Chin. Phys. B* **30** 046801
[25] Li C *et al.* 2019 *Acta Phys. Sin.* **68** 118102 (in Chinese)

Supplementary Material for **"Effect of Oxide Content of Graphene Oxide Membrane on Remarkable Adsorption for Calcium Ions"**

PS1: Method

GO suspension with the concentration of ~4 mg/ml was prepared by the modified Hummers method. Ten-minutes' ultrasonic treatment with the frequency of 70 kHz has been performed to enhance the dispersion of GO sheets. After that, 1 ml GO suspension formed the GOMs via the drop-casting method followed by the drying process at 60℃ for 8 hours. The obtained GOMs are immersed in the 40-ml $CaCl_2$/NaCl solutions of various concentrations at room temperature. The extra $CaCl_2$ and NaCl solution adsorbed on the surface of the GOMs also had been removed by the absorbent paper. Then the obtained $CaCl_2$@GOMs were dried at 60℃ for 12 hours.

The metal ions in the GOMs were determined by inductively coupled plasma optical emission spectroscopy (ICP-OES). The desorption amount of $CaCl_2$/NaCl during immersing $CaCl_2$@GOMs in DI water had been detected by the concentration variation in the solution by using conductance meter.

The prepared $CaCl_2$@GOMs samples were characterized by Siemens XRD and LEO 1530VP SEM operated at 10 kV.

PS2: Reusability of GO membranes

In industrial applications, reusability is used to evaluate the feasibility of an adsorbent. Their reusability was investigated by adsorption and desorption experiment repeated for several times. After adsorption, the GO membranes were desorbed DI

water, and then dried. The GOMs were then placed in a $CaCl_2$ solutions. The adsorption capacity for Ca^{2+} decreased slightly with increasing treatment cycles, but remain 0.425 g/g in the fourth cycle relative. After these cycles, the properties of the GOMs are still stable.

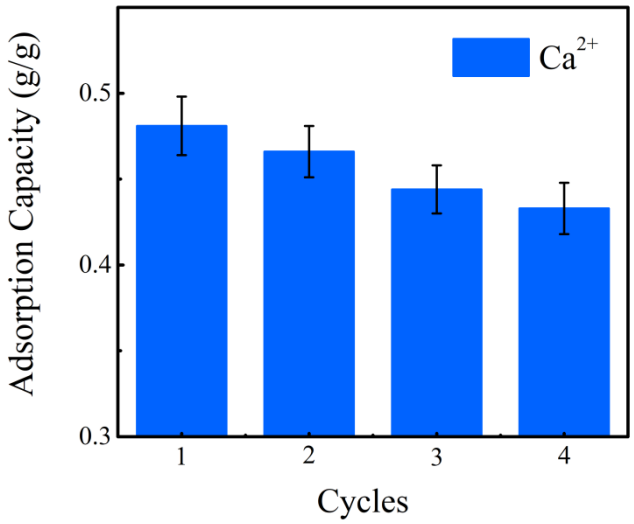

Fig S1: Recycling of GOMs for Ca^{2+} adsorption. Adsorption capacity with respect to the treatment cycles by GOMs. Error bars indicate the standard deviation.

PS3: Case of NaCl@GOMs

The GOMs contained NaCl (NaCl@GOMs) were also prepared via the same synthesis procedure as the case of $CaCl_2$@GOMs. Fig. S2a shows that the adsorption capacity of Na^+ in NaCl@GOMs can be as high as ~0.213 mg/mg after immersing GOMs heat-treated at 60 ℃ in the 6.0 M NaCl solution. It is also shown that the adsorption capacity of Na^+ increases from ~0.099 mg/mg to ~0.213 mg/mg with increases the concentration of NaCl solution from 3.0 to 6.0 M, respectively.

Desorption process of NaCl was also studied via immersing NaCl@GOMs into DI water. The NaCl@GOMs with the adsorption capacity of ~0.213 mg/mg are

chosen to use in our experiments. Similar to the case of $CaCl_2$@GOMs, we find that the desorption process of NaCl can also been divided into three stages as shown in Fig. S2b. The concentration of NaCl in the solution increases rapidly from 0 to 17 ppm in the first 1 min, then slowly to 28 ppm in the range of 1 - 5 min. Afterwards, the concentration of NaCl in the solution becomes stable.

Fig. S2c shows the XRD pattern of NaCl@GOMs and there are several Bragg peaks at different diffraction angles (2θ). The peak at ~11 degree for pristine GOMs and ~12 degree for NaCl@GOMs come from the GOMs. The weak peak at ~28 degree and strong peak at ~32 degree come from the (111) and (200) surface of the ordinary NaCl crystal in the NaCl@GOMs. SEM image shows extensive distribution of NaCl inside NaCl@GOMs, as shown in Fig. S2d. Fig. S2e shows elemental mappings of C, O, Na, Cl elements. We find that the signals of Na and Cl elements in the region covered with large amount of NaCl are shown very high intensities as the intensities of C and O elements, which further confirms the remarkable amount and wide distribution of NaCl in NaCl@GOMs.

Similar to the case of $CaCl_2$@GOMs, the remarkable amount of NaCl adsorbed inside the NaCl@GOMs can also be attributed to strong interactions between NaCl and GO sheets, including the ion-π interactions between Na^+/Cl^- and aromatic graphitic rings as well as the electrostatic interaction between Na and oxide groups. The desorption process of NaCl from NaCl@GOMs is similar to that of $CaCl_2$ from $CaCl_2$@GOMs.

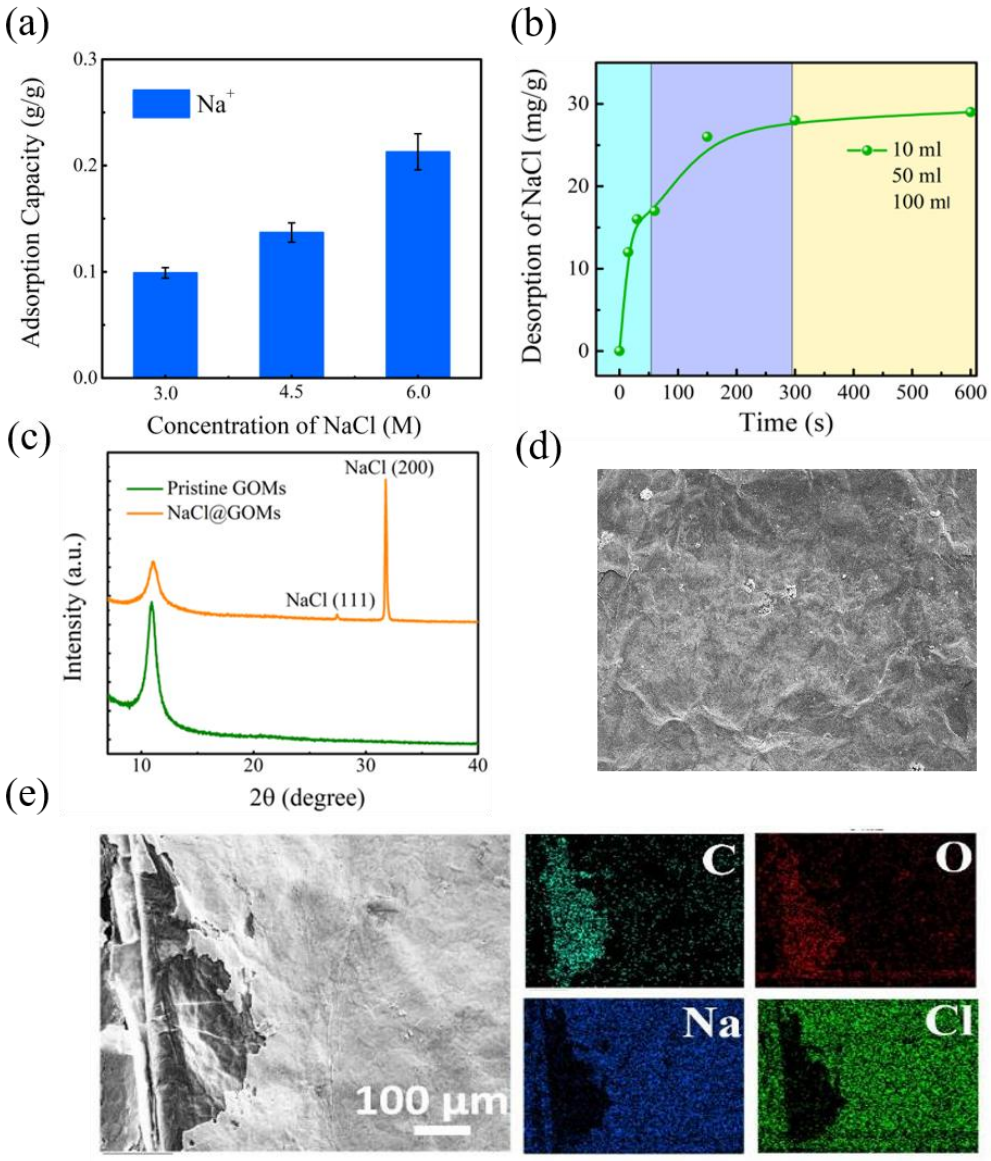

Fig. S2 Case of NaCl@GOMs. (a) Adsorption capacity of NaCl in NaCl@GOMs after immersing NaCl solution. (b) Desorption process of NaCl from NaCl@GOMs after immersing in DI water of 50 ml. The process can be divided into three stages: I. fast desorption stage (cyan-blue region), II. Slow desorption stage (purple region), III. stable stage (yellow region). (c) XRD patterns of NaCl@GOMs (orange line). (d) SEM image of NaCl@GOMs. (e) Elemental mappings of NaCl@GOMs. C, O, Na, Cl elements are displayed as the colors of cyan, red, blue and green, respectively. Error bars indicate the standard deviation.